Theoretical Study of Hydrolysis and Condensation of Silicon Alkoxides

Satoshi Okumoto and Naokatsu Fujita

Matsushita Electric Works, Ltd., 1048, Kadoma, Osaka 571, Japan

Shinichi Yamabe*

Department of Chemistry, Nara University of Education, Takabatake-cho, Nara 630, Japan

Received: January 7, 1998; In Final Form: March 20, 1998

The two title reactions were investigated by means of ab initio molecular orbital calculations. Under neutral conditions, the hydrolysis of methylmethoxydihydroxysilane was examined, and the water-trimer cluster was found to be a reactant for ready bond interchange. The condensation of methyltrihydroxysilane was caused by the participation of the water dimer. Two of the observed reactions involved a front-side nucleophilic attack to the silicon center or a similar mechanism. Acid- and base-promoted hydrolyses were also examined, and their enhanced reactivities were ascribed to the stability of the silyl cation and a hypervalent intermediate, respectively.

I. Introduction

Hydrolysis and the subsequent condensation of alkoxysilanes are industrially important reactions for obtaining ceramics, glasses, and fibers (Scheme 1).[1] The mechanisms for these reactions have been extensively studied by the measurement of kinetics and the examination of catalytic effects.[2−19] For acid- and base-promoted reactions, it has been thought that S_N2-type back-side displacement (inversion) paths are likely. However, the mechanism for hydrolysis and condensation under neutral conditions has remained unclear. For some silicon substrates, retention paths have been suggested.[6] In the investigation of the reaction mechanism, the problem lies in determining how water molecules are involved with both nucleophilic attacks to the silicon center and proton relay for exchanges of covalent (O−H) and hydrogen (O···H) bonds. Concentrations of $[H^+]$ and $[OH^-]$ are 10^{-7} mol/L, respectively, while $[H_2O] \approx 1000/18 = 55.6$ mol/L. Neutral water clusters (dimer, trimer, etc.) should be reactants.

In the present work, ab initio calculations have been performed to examine those reactions under neutral condition. Acid- and base-assisted reactions will also be investigated to compare their paths with those under neutral conditions. Front-side displacements involving cyclic transition states will be shown to control simultaneous proton transfers and the resultant oxygen exchanges.

II. Methods of Computations

Ab initio calculations were performed using the GAUSSIAN 94 [20] program on the CONVEX SPP 1200/XA computer at the Information Processing Center of Nara University of Education and the SGI Indigo2 computer at Matsushita Electric Works, Ltd. RHF/3-21G(*), RHF/6-31G*, and RHF/6-31G*(SCRF)[21] methods were applied to geometry optimizations and subsequent vibrational analyses. Specifically, for an anion system $HO^-(H_2O) + Me\ Si\ OMe(OH)_2$ (in Figure 9), RHF/3-21+G(*) and RHF/6-31+G* were used. Inclusion of diffuse basis functions is indispensable to describing negatively charged systems.[22] Energies were refined by single-point calculations of the density functional theory of B3-LYP[23] on the 6-31G* or 6-31+G* basis set with the SCRF solvent effect.

SCHEME 1

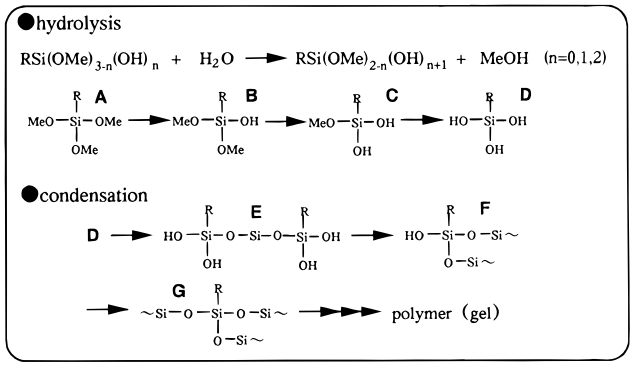

III. Results and Discussions

Neutral Hydrolysis. Figure 1 shows a reaction between methylmethoxydihydroxysilane (**C**) and a water molecule. In **C**, the silicon atom is quite cationic [+1.5], and the oxygen atoms are very anionic [−0.7 to −0.8]. An association complex, "reactant complex (RC)", is obtained, where two Si−O bonds are slightly elongated owing to hydrogen bonds. When the H_2O molecule is rotated in the intermediate, a four-centered transition state, TS, is generated. In the TS, MeOH becomes a good leaving group. After the TS, a second intermediate, "product complex (PC)", is created. In PC, its stability arises from a H···O hydrogen bond (RHF/6-31G*). PC gives the hydrolysis product, **D**, and a methanol molecule.

Figure 2 shows a reaction between **C** and a water dimer. Their association species can be referred to as "RC". In the RC, a hydrogen-bond ring is formed that is ready for the subsequent TS. This ring formation provides a strainless bond interchange. With RHF/6-31G*, only hydrogen bonds (not the Si···O attraction) are involved in the intermediate. The RC intermediate can also be readily isomerized to the TS. The TS then forms an O−H bond, and the Si−OMe bond is cleaved.

S1089-5639(98)00705-1 CCC: $15.00
Published on Web 05/08/1998

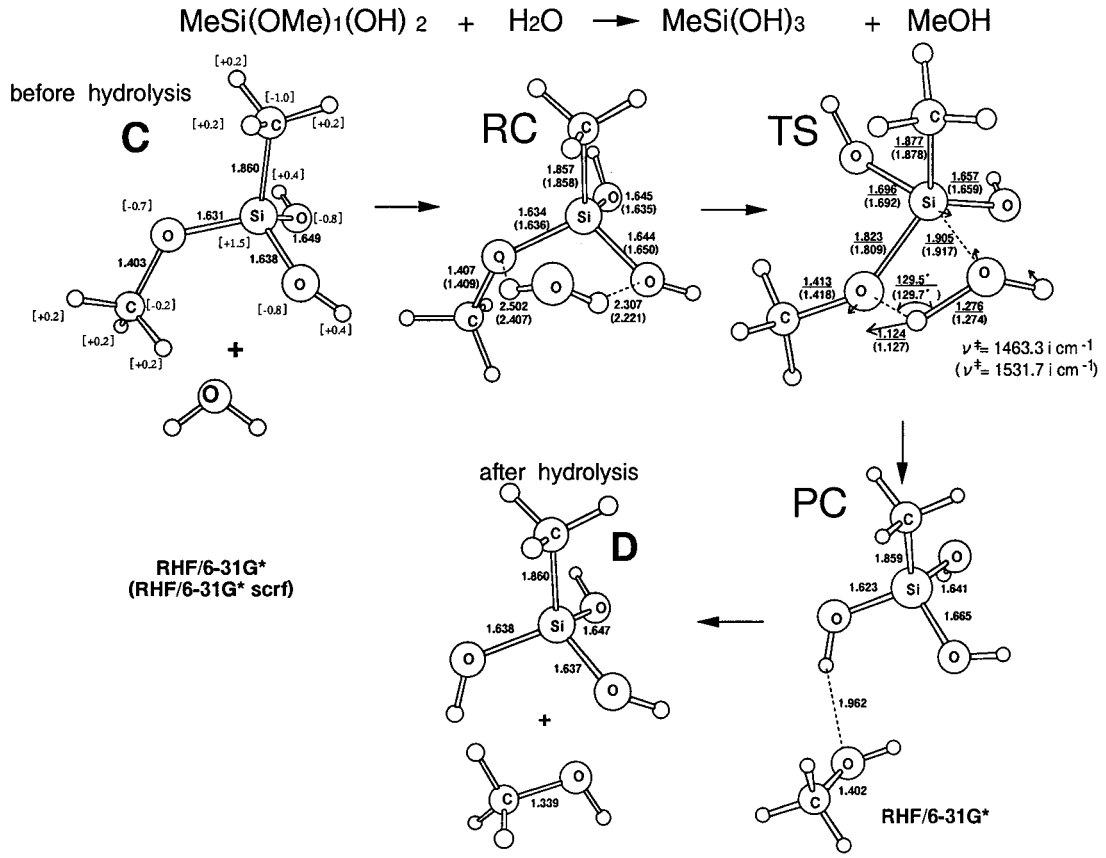

Figure 1. Geometries optimized with three methods for the one-water associated hydrolysis shown in Scheme 1. Empty small circles denote hydrogen atoms. TS is the transition state with a sole imaginary frequency, $\nu^{\ddagger}$. RC is the reactant complex, and PC is the product complex, respectively. Values in square brackets at **C** show RHF/3-21G* Mulliken net charges (positive, cationic). Distances are in angstroms. **C** and **D** are defined in Scheme 1.

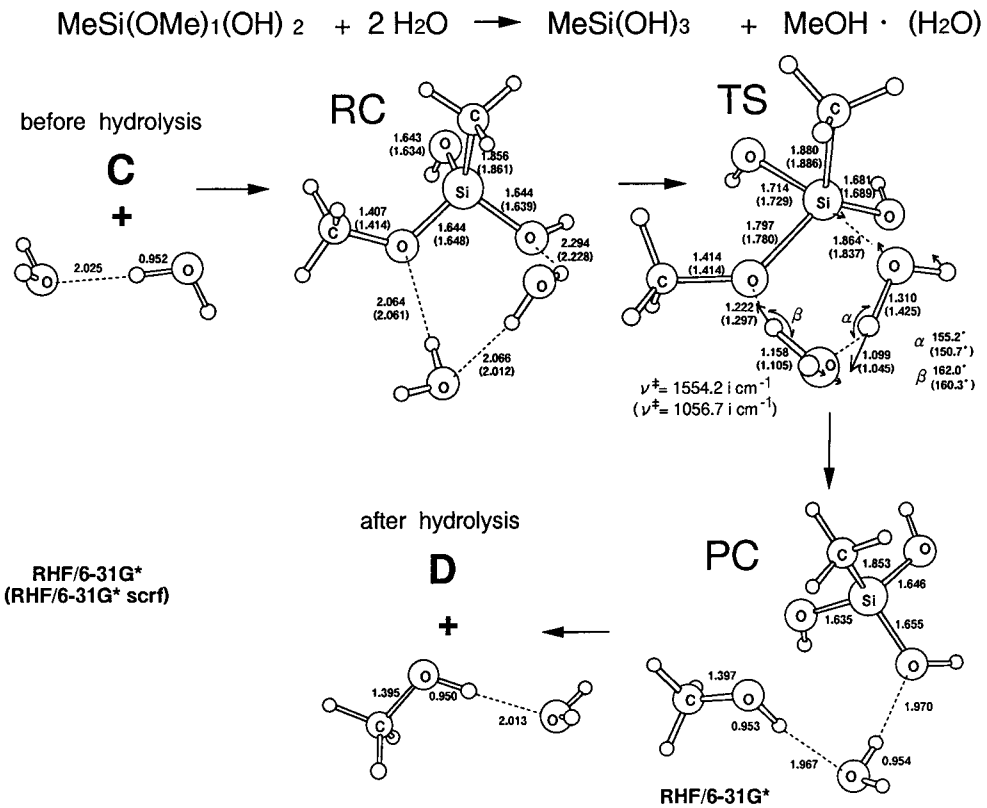

Figure 2. Geometries for the two-water associated hydrolysis shown in Scheme 1. Same notations as in Figure 1 are used. Geometries of **C** and **D** are shown in Figure 1.

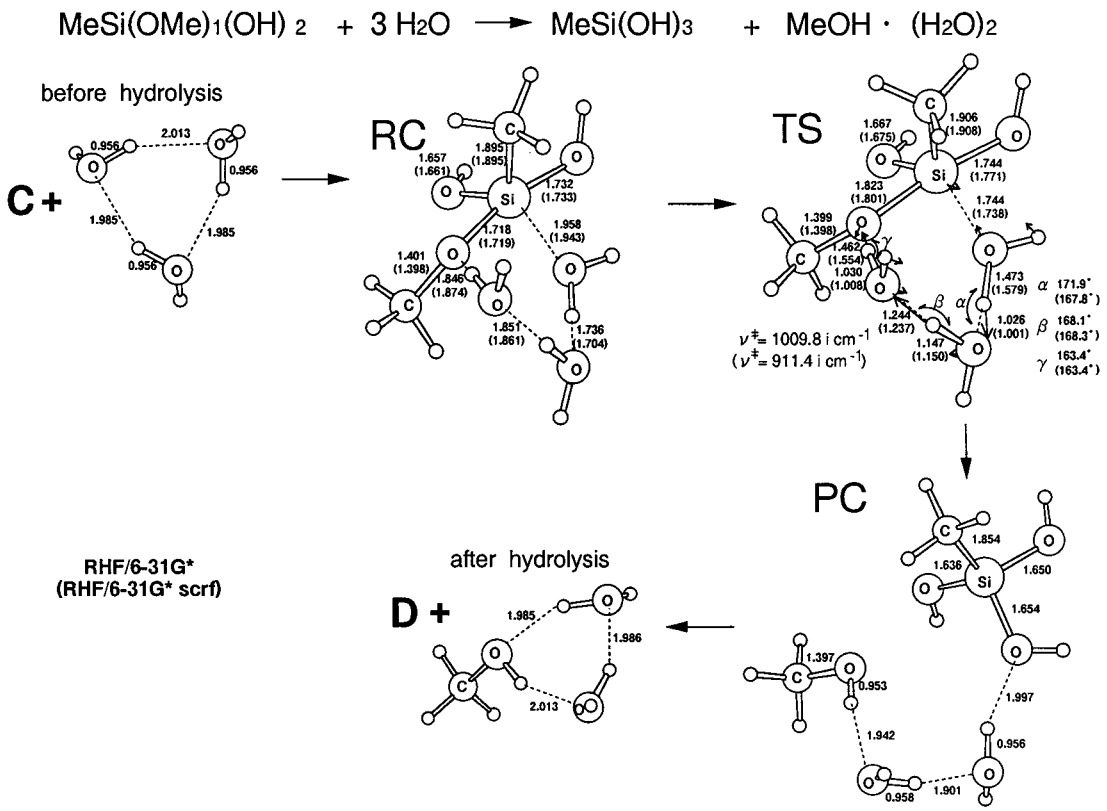

Figure 3. Geometries for the three-water hydrolysis.

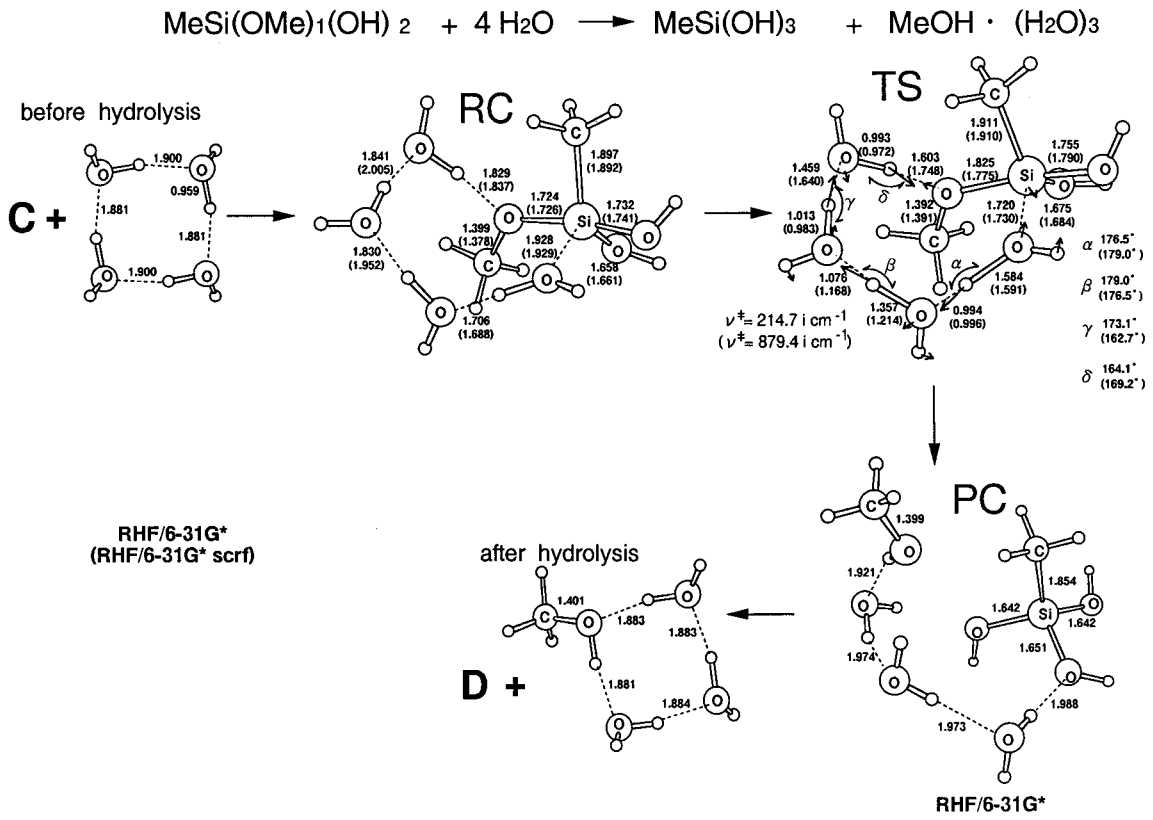

Figure 4. Geometries for the four-water hydrolysis.

After the TS, the second intermediate, "PC", is generated. PC leads to a hydrolyzed product, **D**, and a methanol−water hydrogen-bond complex. Indeed, the shape of the six-membered ring for the TS has a reasonable bond interchange, but the hydrogen-bond angle α is still bent (∼150°, ideally 180°). In order to improve the angle (toward 180°), one more water molecule is added as a reactant. That is, the substrate **C** and a water trimer are combined, as shown in Figure 3. It is noteworthy that two computational methods give a cyclic geometry for RC, which is close to that of the subsequent TS. The

TABLE 1: Total Energies (in hartrees) and Their Differences (in kcal/mol, parentheses) Relative to Those of Reactant Complex for Hydrolysis (Neutral Condition)[a]

n	method	before hydrolysis	RC	TS	PC	after hydrolysis
1 (Figure 1)	RHF/3-21G*	−666.5847 (12.5)	−666.6045(0)	−666.5714 (20.8)	−666.5760 (18.0)	−666.5872 (14.1)
	RHF/6-31G*	−670.0551 (5.5)	−670.0638 (0)	−669.9983 (41.1)	−670.0712 (−4.6)	−670.0564 (4.7)
	free energy	−669.9676 (−4.4)	−669.9606 (0)	−669.8914 (43.4)	−669.9663 (−3.6)	−669.9695 (−5.6)
	RHF/6-31G*(scrf)		−670.0675 (0)	−669.9999 (42.5)		
	B3-LYP/6-31G*(scrf) //RHF/6-31G*		−672.7476 (0)	−672.7047 (26.9)	−672.7563 (−5.5)	
2 (Figure 2)	RHF/3-21G*	−742.1881 (18.8)	−742.2181 (0)	−742.2017 (10.3)	−742.2236 (−3.5)	−742.1908 (17.1)
	RHF/6-31G*	−746.0748 (6.4)	−746.0850 (0)	−746.0210 (40.2)	−746.0879 (−1.8)	−746.0761 (5.6)
	free energy	−745.9698 (−6.5)	−745.9595 (0)	−745.8902 (43.5)	−745.9626 (−2.0)	−745.4713 (−7.4)
	RHF/6-31G*(scrf)		−746.0953 (0)	−746.0241 (44.7)		
	B3-LYP/6-31G*(scrf) //RHF/6-31G*		−749.1711 (0)	−749.1394 (19.9)	−749.1744 (−2.1)	
3 (Figure 3)	RHF/3-21G*	−817.8130 (12.0)	−817.8322 (0)	−817.8304 (1.1)	−817.8451 (−8.1)	−817.8146 (11.0)
	RHF/6-31G*	−822.1044 (−18.1)	−822.0755 (0)	−822.0460 (18.5)	−822.1113 (−22.4)	−822.1054 (−18.8)
	free energy	−821.9736 (−35.1)	−821.9177 (0)	−821.8903 (17.2)	−821.9644 (−29.3)	−821.9748 (−35.8)
	RHF/6-31G*(scrf)		−822.0769 (0)	−822.0527 (15.2)		
	B3-LYP/6-31G*(scrf) //RHF/6-31G*		−825.5757 (0)	−825.5715 (2.7)	−825.5978 (−13.8)	
4 (Figure 4)	RHF/3-21G*	−893.4374 (8.8)	−893.4514 (0)	−893.4491 (1.5)	−893.4640 (−7.9)	−893.4409 (6.6)
	RHF/6-31G*	−898.1328 (−19.8)	−898.1013 (0)	−898.0673 (21.3)	−898.1409 (−24.9)	−898.1354 (−21.4)
	free energy	−897.9796 (−36.2)	−897.9216 (0)	−897.8853 (22.8)	−897.9676 (−28.9)	−897.9813 (−37.5)
	RHF/6-31G*(scrf)		−898.1034 (0)	−898.0801 (14.6)		
	B3-LYP/6-31G*(scrf) //RHF/6-31G*		−902.0027 (0)	−901.9980 (3.0)	−902.0350 (−20.3)	

[a] Gibbs free energies (RHF/6-31G*) are at $T = 298.15$ K. RHF/3-21G* geometries are not shown in Figures 1−4 for clarity.

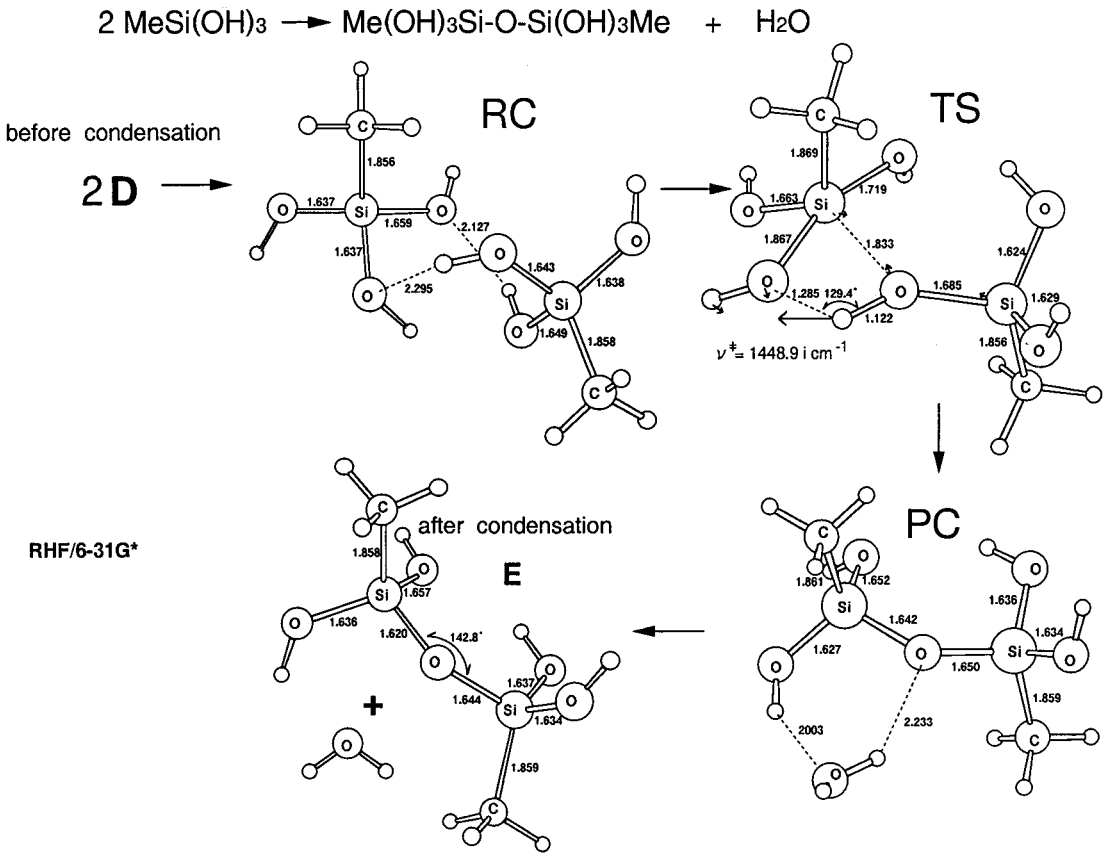

Figure 5. Geometries for the water-free condensation shown in Scheme 1.

network formation occurs almost simultaneously with the hydrolysis reaction. Next, a water tetramer is tested for the reaction shown in Figure 4. Almost linear hydrogen bonds are involved at the TS. Here, the H_2O tetramer appears to be the best reactant for hydrolysis.

In Table 1,[24] energy barrier heights are compared. The $n = 3$ activation energy is smallest with B3-LYP/6-31G*(SCRF), which indicates that the water trimer is the best reactant. Indeed the tetramer has linear hydrogen bonds, but the O−H covalent bonds concerned with them deviate from oxygen lone-pair orbitals. Because participation of the water trimer in the silicon front-side attack is reasonable geometrically, a likely stereochemistry in hydrolyses would involve the retention of the Si tetrahedron.

Neutral Condensation. Figure 5 shows a condensation reaction of two methyltrihydroxysilanes (**D**'s). First, a dimer **D**···**D**,

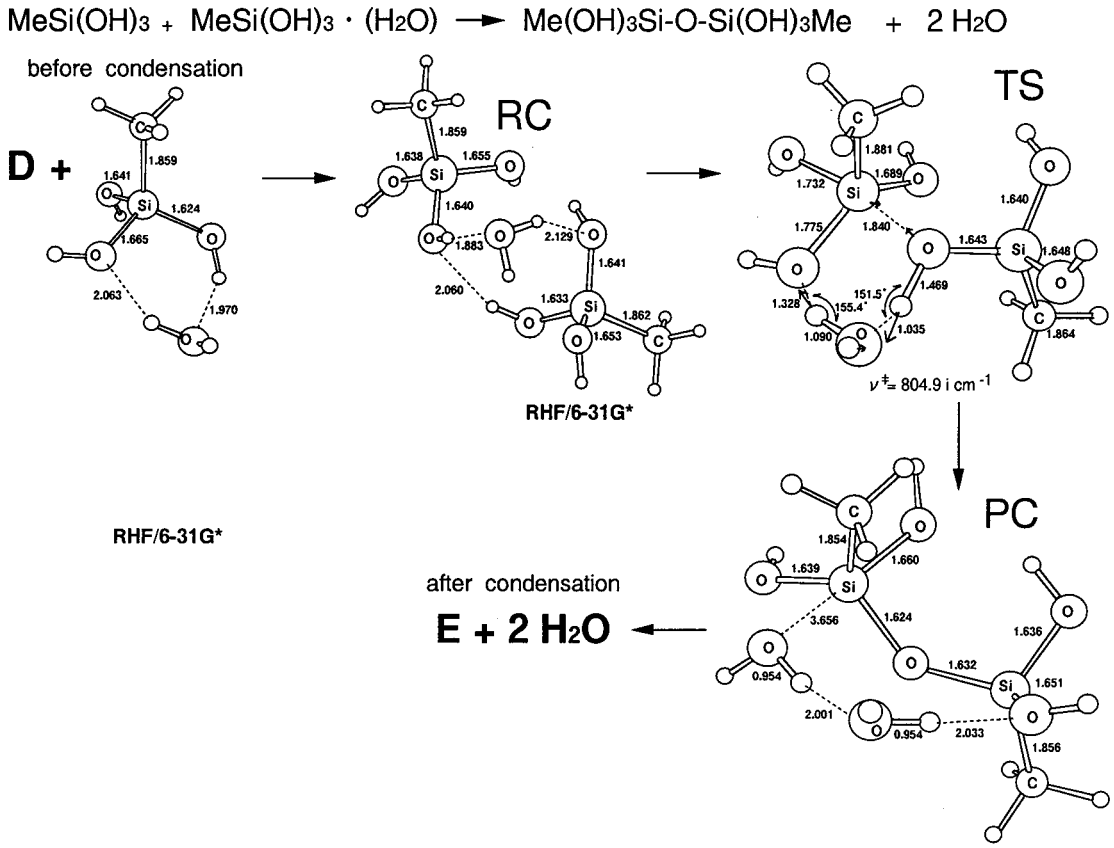

Figure 6. Geometries for the one-water associated condensation.

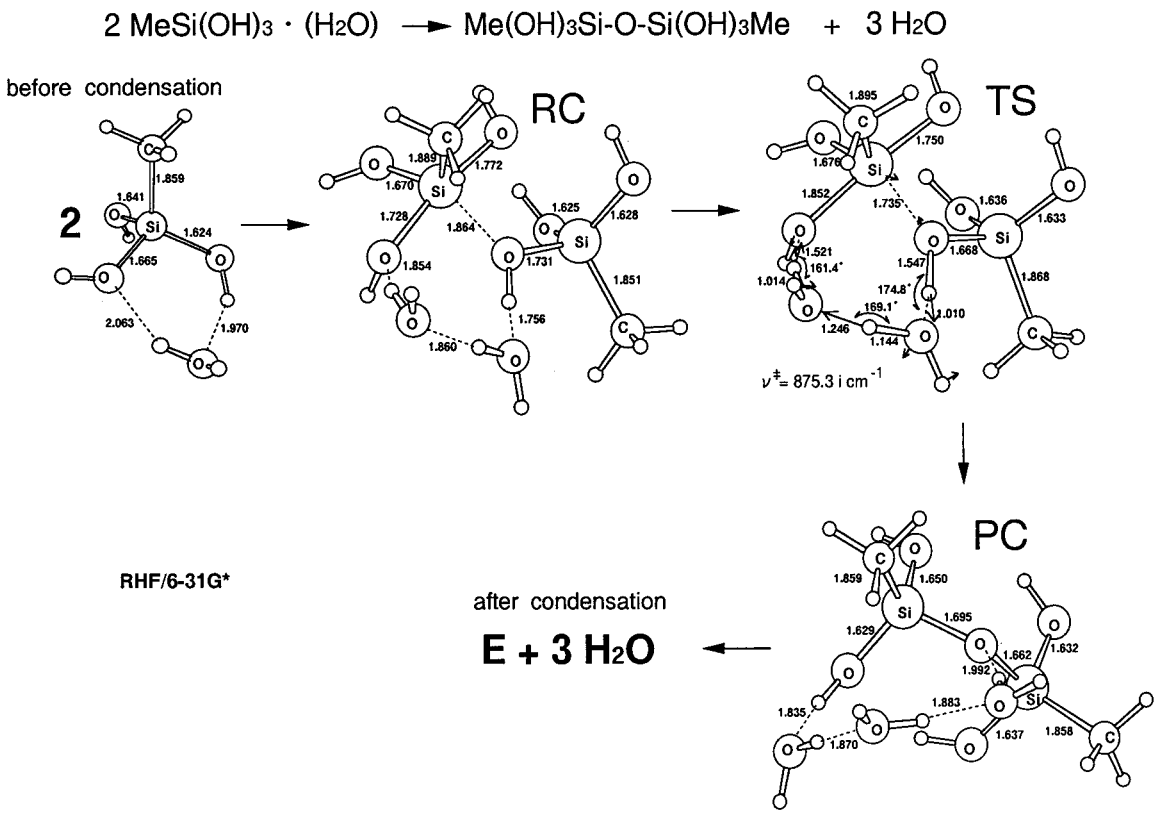

Figure 7. Geometries for the two-water associated condensation.

RC, is generated. Through the deformation of the dimer, a four-center transition state, the TS, is obtained. After the TS, a complex (PC) between the condensed product **E** and a water molecule is attained. The reaction pattern is similar to that involving the hydrolysis of $(H_2O)_1$ participation, as shown in Figure 1.

TABLE 2: Total Energies (in hartrees) and Their Differences (in kcal/mol, Parentheses) Relative to Those of Reactant Complex for Condensation (Neutral Condition)[a]

n	method	before condensation	RC	TS	PC	after condensation
0 (Figure 5)	RHF/3-21G*	−1104.3784 (19.4)	−1104.4093 (0)	−1104.3709 (24.1)	−1104.4032 (3.8)	−1104.3927 (10.4)
	RHF/6-31G*	−1110.0420 (9.5)	−1110.0572 (0)	−1109.9884 (43.2)	−1110.0659 (−5.5)	−1110.0524 (3.0)
	free energy	−1109.9335 (−24.4)	−1109.9273 (0)	−1109.8569 (44.2)	−1109.9370 (−26.6)	−1109.9403 (−28.7)
	B3-LYP/6-31G*(scrf) //RHF/6-31G*		−1114.0656 (0)	−1114.0182 (29.8)	−1114.0710 (−3.3)	
1 (Figure 6)	RHF/3-21G*	−1179.9949 (13.4)	−1180.0163 (0)	−1180.0358 (8.3)	−1180.0358 (−12.2)	−1179.9996 (12.7)
	RHF/6-31G*	−1186.0678 (10.3)	−1186.0843 (0)	−1186.0165 (42.5)	−1186.0855 (−0.8)	−1186.0722 (7.6)
	free energy	−1185.9363 (−1.6)	−1185.9336 (0)	−1185.8587 (47.0)	−1185.9346 (−0.6)	−1185.9426 (−5.7)
	B3-LYP/6-31G*(scrf) //RHF/6-31G*		−1190.4946 (0)	−1190.4538 (25.6)	−1190.4910 (2.2)	
2 (Figure 7)	RHF/3-21G*	−1255.6115 (15.2)	−1255.6357 (0)	−1255.6338 (1.2)	−1255.6604 (−15.4)	−1255.6210 (9.2)
	RHF/6-31G*	−1262.0936 (−15.1)	−1262.0696 (0)	−1262.0424 (17.1)	−1262.1186 (−30.8)	−1262.1017 (−20.1)
	free energy	−1261.9391 (1.3)	−1261.8863 (0)	−1261.8595 (16.8)	−1261.9426 (−35.3)	−1261.9464 (−37.7)
	B3-LYP/6-31G*(scrf) //RHF/6-31G*		−1266.8926 (0)	−1266.8903 (1.4)	−1266.9305 (−23.8)	

[a] Gibbs free energies (RHF/6-31G*) are at $T = 298.15$ K. RHF/3-21G* geometries are not shown in Figures 5−7 for clarity.

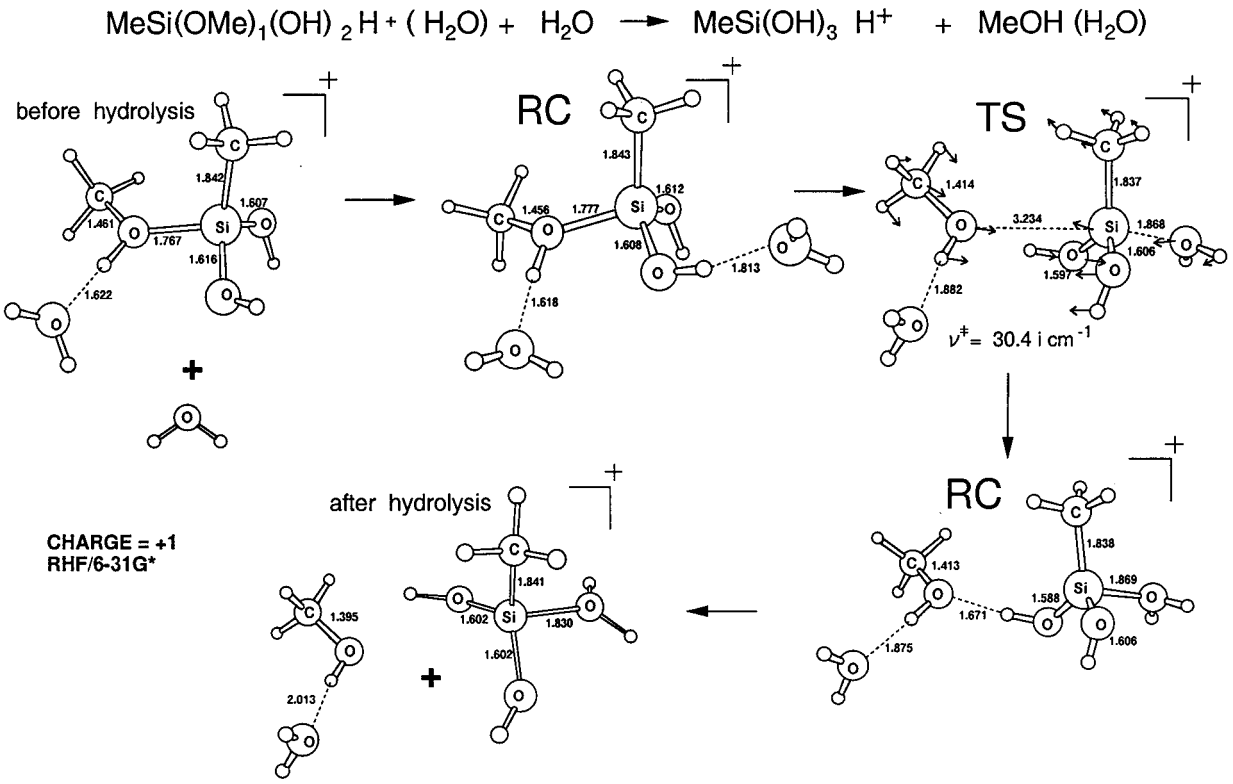

Figure 8. Geometries for an acid-catalyzed hydrolysis.

Figure 6 presents a condensation model between **D** and **D**···H_2O. This complex, RC, has a ring-shaped hydrogen-bond network. Simultaneous proton transfer and Si···O approach lead to the transition state, TS. There are many hydrogen-bond configurations of RC by RHF/6-31G*. These configurations, one of which is shown in Figure 6, apparently do not correspond to the subsequent TS. Of course, versatile hydrogen bonds may be readily broken by thermal energy, and the TS may be arrived at by small geometric distortions. The six-membered cyclic form of the TS is very close to that of the two-water accompanied TS of hydrolysis (Figure 2), but the hydrogen-bond linearity is insufficient. One more water molecule is needed to cause facile proton transfer. In Figure 7, this model is tested. When two substrates, both of which are solvated by water molecules, interact with each other, a ring strain-free network is attained at the TS. The geometry most likely for condensation is similar to that for the hydrolysis shown in Figure 3. In fact, the energy barrier height of $n = 2$ is lowest for the condensation (Table 2). Thus, hydrolyses and condensations under neutral conditions have the same reaction patterns, with a silicon front-side nucleophilic attack and concomitant bond interchanges. The linearity and directionality of the hydrogen bonds involved must be assured.

Reactivities of the hydrolysis and condensation are compared. In Table 1, the $n = 3$ hydrolysis TS has been found to have the smallest energy barrier height. In Table 2, the $n = 2$ condensation TS is the smallest. These two barrier heights do not differ significantly (e.g., 2.7 kcal/mol of $n = 3$ of hydrolysis and 1.4 kcal/mol of $n = 2$ of condensation by B3-LYP/6-31G*-(SCRF)). When the activation energies are similar, the difference in the rate constants can be ascribed to collisional efficiency. Under usual experimental conditions, molar concentrations are $[H_2O] \gg$ [silicon substrate]. Therefore, the hydrolysis takes place first (Figure 3). All the methoxy groups in silicon substrates are replaced by hydroxy groups. After and even during hydrolysis, hydroxy groups are exchanged between

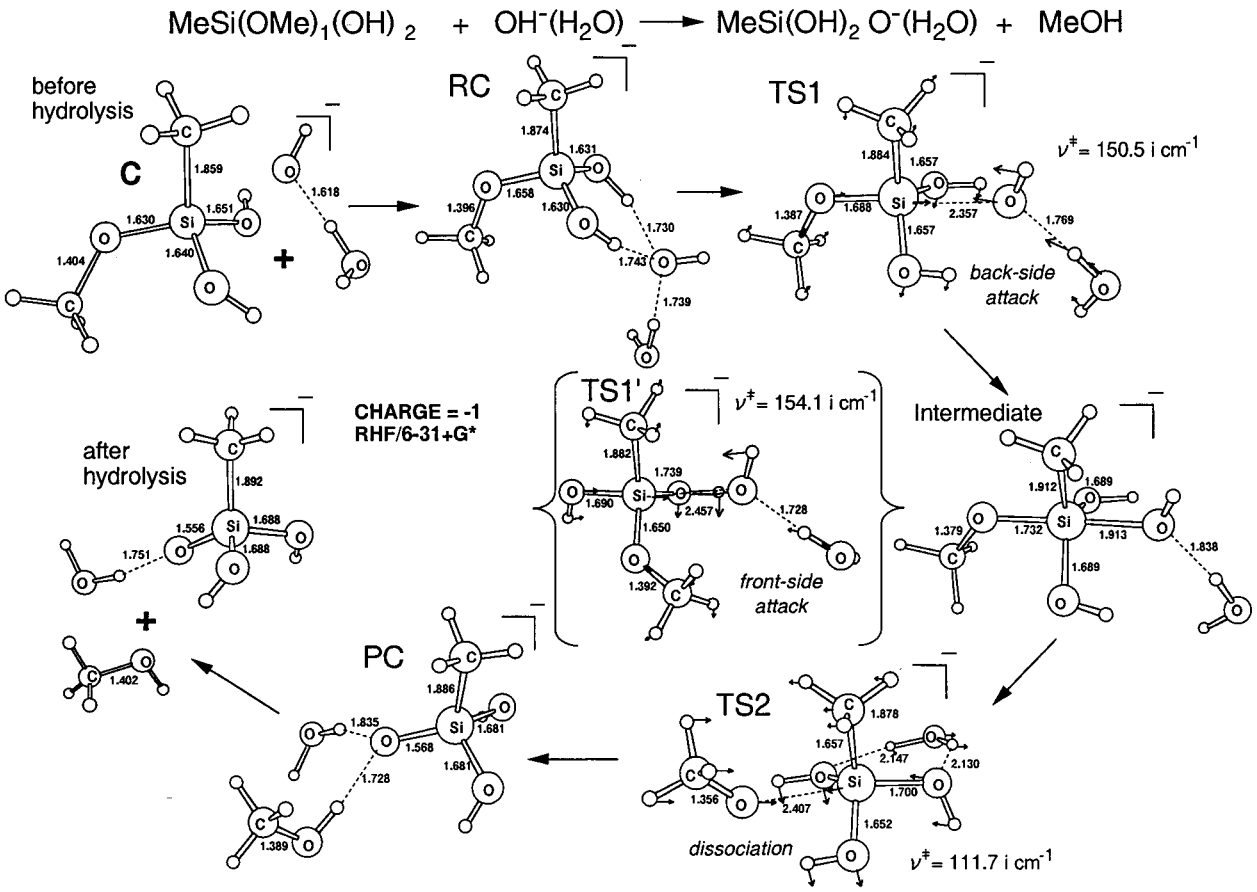

Figure 9. Geometries for a base-promoted hydrolysis.

TABLE 3: Total Energies (in hartrees) and Their Differences (in kcal/mol, Parentheses) Relative to Those of Reactant Complex for Hydrolysis on (a) Acid and (b) Base Conditions[a]

(a) Hydrolysis (Acid Condition)

method	before hydrolysis	RC	TS	PC	after hydrolysis
RHF/3-21G*	−742.5781 (25.2)	−742.6183 (0)	−742.5803 (23.8)	−742.5853 (20.7)	−742.5252 (58.4)
RHF/6-31G	−746.4281 (14.9)	−746.4519 (0)	−746.4278 (15.1)	−746.4283 (14.8)	−746.3903 (38.6)
B3-LYP/631G*(scrf)//RHF/6-31G*		−749.5391 (0)	−749.5172 (13.7)	−749.5178 (13.3)	

(b) Hydrolysis (Base Condition)

method	before hydrolysis	RC	TS1	TS1′
RHF/3-21(+)G*	−741.7319 (41.1)	−741.7973 (0)	−741.7846 (8.0)	−741.7752 (13.9)
RHF/6-31(+)G*	−745.4903 (40.1)	−745.5541 (0)	−745.5441 (6.3)	−745.5316 (14.1)
B3-LYP/6-31G*(scrf)//RHF/6-31G*		−748.6832 (0)	−748.6672 (10.0)	−748.6542 (18.1)

method	intermediate	TS2	PC	after hydrolysis
RHF/3-21(+)G*	−741.7894 (5.0)	−741.7781 (12.1)	−741.8007 (−2.1)	−741.7694 (17.5)
RHF/6-31(+)G*	−745.5479 (3.9)	−745.5436 (6.6)	−745.5665 (−7.8)	−745.5410 (8.2)
B3-LYP/6-31G*(scrf)//RHF/6-31G*	−748.6670 (10.1)	−748.6646 (11.7)	−748.6843 (−0.7)	

[a] RHF/3-21G* geometries are not shown for clarity.

water clusters and silicon substrates, and an equilibrium is achieved. During the course of these OH exchanges, there is a low probability that intermediate **3** (Figure 7) will be generated. Noteworthy is that the exothermicity of the B3-LYP/6-31G*-(SCRF) RC → PC ($n = 2$, −23.8 kcal/mol in Table 2) is larger than that of the RC → PC ($n = 3$, −13.8 kcal/mol in Table 1). PCinvolves an MeOH methyl (hydrophobic) group interfering with a hydrogen-bond network. In spite of the low probability of RC occurring, the thermodynamically stable intermediate (PC) will gradually be yielded.

Although calculations cannot directly deal with reactions in aqueous media, the present results showing the involvement of hydrogen bonds seem to be useful in analyzing reaction mechanisms.

Hydrolyses of Charged Substrates. Figure 8 presents a model of an acid-catalyzed hydrolysis. A proton solvated by a water molcule is added to the substrate, **D**. When the methoxy oxygen atom is protonated, the Si−O distance increases (1.642 Å → 1.767 Å by RHF/6-31G*). Even without the nucleophile H_2O, the protonated species is regarded as a complex between a methanol molecule and a silyl cation. The nucleophile naturally attacks the less-crowded back-side of the cation in the S_N2 manner. Normally, a specific activation energy is necessary tobreak the Si−O bond, but the protonation (strictly

SCHEME 2

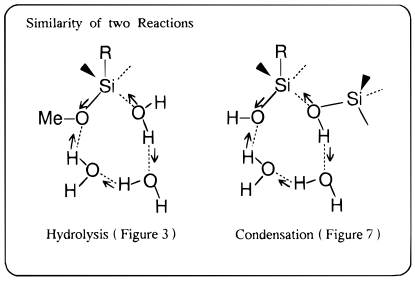

speaking, proton transfer from a cation source via the hydrogen-bond network) weakens the Si−O bond prior to the nucleophilic attack. In fact, the absolute values of sole imaginary frequencies (78.1i cm^{-1} by RHF/3-21G* and 30.4i cm^{-1} by RHF/6-31G*) are extremely small. Thus, the acid-catalyzed hydrolysis occurs quite readily, as was stated in the Introduction.

Figure 9 presents a model of a base-promoted hydrolysis. A hydroxide ion (OH^-) is employed as a nucleophile. Back-side (TS1) and front-side (TS1′) attacks are examined. TS1 is found to have a smaller activation energy by 8.1 kcal/mol (B3-LYP/6-31+G*(SCRF)//RHF/6-31+G*) than TS1′. The back-side attack in the base-promoted hydrolysis has been confirmed. After TS1, a hypervalent intermediate (intermediate such as PCl_5) is formed. The intermediate is decomposed via TS2 to a methanol molecule and a monoanion of trihydroxymethylsilane. The base-promoted hydrolysis is then complete. The high reactivity of charged hydrolyses can be ascribed to the stability of the silyl cation and the anionic hypervalent species.

Table 3 shows the energies of hydrolyses of charged species. In Table 3a, the energy barrier height of TS1 (15.1 kcal/mol by RHF/6-31G*) is very close to the desolvation energy (14.9 kcal/mol) relative to the energy of RC. The similarity demonstrates that the activation energy arises not from S_N2 bond interchange but from desolvation. That is, the energy in the aqueous media would be quite small. In Table 3b, the more drastic difference between 6.3 kcal/mol (TS1) and 40.1 kcal/mol (before hydrolysis) with RHF/6-31(+)G* is noteworthy. The reactivity of charged hydrolyses is controlled not by structural changes of the substrate but by the solvation strength in the present model systems. If hydroxy groups of the substrate are solvated by other water clusters, the activation energies are very small. Thus, charged hydrolyses are more reactive than neutral ones.

IV. Concluding Remarks

This work has dealt theoretically with hydrolysis and condensation of alkoxysilanes. In aqueous media, there are many kinds of water clusters. Some of these clusters may fit the bond interchange through the hydrogen-bond network. The present model calculation seems to provide some insight into reactions in aqueous media. Scheme 2 summarizes computational results for two reactions under the neutral conditions. Under these conditions, hydrolysis and condensation have similar reaction patterns. Front-side nucleophilic attacks have been demonstrated, which is in contrast with the back-side attacks in acid- or base-promoted hydrolysis.

Supporting Information Available: Cartesian coordinates of optimized geometries of all the species shown in Figures 1−9 are displayed together with total and nuclear repulsion energies (48 pages). Ordering information is given on any current masthead page.

References and Notes

(1) (a) Brinker, C. J.; Clark, D. E.; Ulrich, D. R. *Mater. Res. Soc. Symp.* **1984**, 32. (b) Sugahara, Y.; Takeda, Y.; Kuroda, K.; Kato, C. *J. Non-Cryst. Solids* **1988**, *100*, 542.

(2) Aelion, R.; Loebel, A.; Eirich, F. *J. Am. Chem. Soc.* **1950**, *72*, 5705.

(3) Aelion, R.; Loebel, A.; Eirich, F. *Recl. Trav. Chim. Pays-Bas* **1950**, *69*, 61.

(4) Voronkov, M. G.; Mileshkevich, V. P.; Yuzhelevski, Y. A. *The Siloxane Bond*; Consultants Bureau: New York, 1978.

(5) McNeill, K. J.; DiCaprio, J. A.; Walsh, D. A.; Pratt, R. F. *J. Am. Chem. Soc.* **1980**, *102*, 1859.

(6) (a) Keefer, K. D. In *Matter Ceramics Through Chemistry*; Brinker, C. J., Clark, D. E., Ulrich, D. R., Eds.; North-Holland: New York, 1984; p 15. (b) Pohl, E. R.; Osterholtz, F. D. *Molecular Characterization of Composite Interfaces*; Ishida, H., Kumar, G., Eds.; Plenum: New York, 1985; p 157.

(7) Pope, E. J. A.; Mackenzie, J. D. *J. Non-Cryst. Solids* **1986**, *87*, 185.

(8) Nishiyama, N.; Horie, K.; Asakura, T. *J. Appl. Polym. Sci.* **1987**, *34*, 1619.

(9) Pouxviel, J. C.; Boilot, J. P. *J. Non-Cryst. Solids* **1987**, *94*, 374.

(10) Kay, B. D.; Assink, R. A. *J. Non-Cryst. Solids* **1988**, *99*, 359; **1988**, *104*, 112; **1988**, *107*, 35.

(11) Nishiyama, N.; Asakura, T.; Horie, K. *J. Colloid Interface Sci.* **1988**, *124* (1), 14.

(12) Nishiyama, N.; Horie, K.; Asakura, T. *J. Colloid Interface Sci.* **1989**, *129* (1), 113.

(13) Yang, H.; Ding, Z.; Jiang, Z.; Xu, X. *J. Non-Cryst. Solids* **1989**, *112*, 449.

(14) Ro, J. C.; Chung, J. *J. Non-Cryst. Solids* **1989**, *110*, 26.

(15) Hench, L. L.; West, J. K. *Chem. Rev.* **1990**, *90*, 33.

(16) Brinker, C. J.; Schere, G. W. *Sol-Gel Science*; Academic Press: Boston, 1990; p 97.

(17) Sanchez, J.; McCormick, A. *J. Phys. Chem.* **1992**, *96*, 8973.

(18) Wen, J.; Mark, J. E. *Polym. Prepr., Am. Chem. Soc. Div. Polym. Chem.* **1993**, *34* (2), 362.

(19) Liu, J.; Kim, S. D. *J. Polym. Sci., Part B: Polym. Phys.* **1996**, *34*, 131.

(20) Frisch, M. J.; Trucks, G. W.; Schlegel, H. B.; Gill, P. M. W.; Johnson, B. G.; Robb, M. A.; Cheeseman, J. R.; Keith, T. A.; Petersson, G. A.; Montogomery, J. A.; Raghavachari, K.; Al-Laham, M. A.; Zakrzewski, V. G.; Ortiz, J. V.; Foresman, J. B.; Cioslowski, J.; Stefanov, B. B.; Nanayakkara, A.; Challacombe, M.; Peng, C. Y.; Ayala, P. Y.; Chen, W.; Wong, M. W.; Andres, J. L.; Replogle, E. S.; Gomperts, R.; Martin, R. L.; Fox, D. J.; Binkley, J. S.; Defrees, D. J.; Baker, J.; Stewart, J. P.; Head-Gordon, M.; Gonzalez, C.; Pople, J. A. *Gaussian 94*, Revision A.1; Gaussian, Inc.: Pittsburgh, PA, 1995.

(21) Onsager, L. *J. Am. Chem. Soc.* **1938**, *58*, 1486.

(22) Clark, T.; Chandrasekhar, J.; Spitznagel, G. W.; Shleyer, P. v. R. *J. Comput. Chem.* **1983**, *4*, 294.

(23) Becke, A. D. *J. Chem. Phys.* **1993**, *98*, 5648.

(24) In $n = 3$ and 4 of "before hydrolysis" of Table 1, energy differences of RHF/3-21G* are positive, while those of RHF/6-31G* are negative. This basis-set dependence comes from the strength of the Si···O intermolecular attraction. The RHF/3-21G* attraction is much stronger than the RHF/6-31G* one. For example, the RHF/3-21G* distance is 1.793 Å, while the RHF/6-31G* one is 1.958 Å. Thus, the stability of the RC is overestimated by RHF/3-21G*.